

MADWAVE3: a quantum time dependent wave packet code for nonadiabatic state-to-state reaction dynamics of triatomic systems .

Octavio Roncero^{a,*}, Pablo del Mazo-Sevillano^b

^a*Instituto de Física Fundamental (IFF-CSIC), Serrano 123, 28006 Madrid (Spain)*

^b*Unidad Asociada UAM-IFF-CSIC, Departamento de Química Física Aplicada, Facultad de Ciencias M-14, Universidad Autónoma de Madrid, 28049 Madrid (Spain)*

Abstract

We present MADWAVE3, a FORTRAN90 code designed for quantum time-dependent wave packet propagation in triatomic systems. This program allows the calculation of state-to-state probabilities for inelastic and reactive collisions, as well as photodissociation processes, over one or multiple coupled diabatic electronic states. The code is highly parallelized using MPI and OpenMP. The execution requires the potential energy surfaces of the different electronic states involved, as well as the transition dipole moments for photodissociation processes. The formalism underlying the code is presented in section 2, together with the modular structure of the code. This is followed by the installation procedures and a comprehensive list and explanation of the parameters that control the code, organized within their respective namelists.

Finally, a case study is presented, focusing on the prototypical reactive collision $\text{H} + \text{DH}(v, j) \rightarrow \text{H}_2(v', j') + \text{D}$. Both the potential energy surface and the input files required to reproduce the calculation are provided and are available on the repository's main page. This example is used to study the parallelization speedup of the code.

NEW VERSION PROGRAM SUMMARY

Program Title: MADWAVE3

CPC Library link to program files: (to be added by Technical Editor)

Developer's repository link: <https://github.com/qmolastro/madwave3>

*Corresponding author.

E-mail address: octavio.roncero@csic.es

Code Ocean capsule: (to be added by Technical Editor)

Licensing provisions(please choose one): GPLv3

Programming language: Fortran 90 *External libraries:* FFTW3, MPI

Supplementary material:

Nature of problem: Quantum time propagation of a wave packet describing a reactive process in a triatomic systems, for collisions (inelastic and reactive) and photodissociation processes, and considering several coupled diabatic electronic state

Solution method(approx. 50-250 words): A modified Chebyshev propagator is used, keeping the real Chebyshev components, which are represented in grids for the internal Jacobi coordinates r, R and γ and in a basis for electronic and helicity components. The potential represented in a grid as well as the reactants and products wave functions are previously calculated in a preparatory stage.

Additional comments including restrictions and unusual features (approx. 50-250 words):

Keywords: Quantum wave packet, reactive collisions, photodissociation, state to state probabilities.

1. Introduction

MADWAVE3 is a code written in FORTRAN90 to treat quantum state-to-state reaction dynamics for $A+BC(v,j) \rightarrow AB(v',j')+C$ collisions and $ABC+h\nu \rightarrow AB(v',j')+C$ photodissociation processes. The code is parallelized using MPI and OpenMP, and this is done primarily on the helicity quantum number, as described below [1]. Non-adiabatic processes are also included by considering multiple electronic states in a diabatic representation, in which the couplings are only due to potential terms, and kinetic coupling terms are neglected.

MADWAVE3 comes with a set of helper programs in order to prepare the calculations, such as generating the potential energy surface grids, and to analyze the results, such as calculating the process cross sections.

To extract the state-to-state probabilities, the Jacobi coordinates of the reactants or products can be used, depending on the masses involved and the symmetry of the reaction [2]. In the reactant Jacobi coordinate based (RCB) method, the wave packet is transformed from the coordinates of the reactants to the coordinates of the products in a sequential procedure at each

iteration, in order to reduce computational time [2]. When using products' coordinates, the transformation is done only once for the initial wave packet.

One popular alternative to run reactive collisions is the ABC code [3]. ABC is a time-independent close-coupling code using hyperspherical coordinates for A+BC reactive collisions, and is easier to converge at low energies and for narrow resonances. However, it scales as n^2 in memory and as n^3 in computing time with the number of channels, n . This is the case for high angular momentum requiring high helicities and for deep insertion wells, where the basis formed by all rearrangement products is sometimes insufficient to converge the calculations. In such a situation, MADWAVE3 is an interesting alternative which scales better with the number of channels since it deals with the calculation of one column of the whole S-matrix. Moreover, MADWAVE3 is highly parallelizable, as commented below, and considers the case of multiple coupled electronic states and can treat photodissociation dynamics, not implemented in the ABC code.

A very popular code for studying photodissociation processes is the time-dependent MCTDH[4, 5, 6] program, which scales very well with increasing system size, since it uses mono-dimensional functions to expand the full wave functions. This allows accurate calculations of the photodissociation cross section, for large systems and including multiple coupled electronic states. However, when the wave packet splits in many portions it is very difficult to converge the basis formed by products of monodimensional functions and there are only few calculations of reactive collisions using MCTDH code.

An alternative is the use of the MCTDH approach within the framework of the thermal flux operator [7, 8] to calculate thermal rate constants in reactions involving polyatomic molecules. This method has been extended to treat state-to-state reaction dynamics in polyatomic systems [9] showing their power. However, this approach is limited to reactions with barriers. In this regard, MADWAVE3 can treat reactions without barriers but is limited to reactions with three atoms or using reduced dimension models for larger systems.

The DIFFREALWAVE[10] code is similar to MADWAVE3, and it is designed to calculate state-to-state differential cross sections in atom plus diatom reactive collisions. This program uses product Jacobi coordinates and one single electronic state. This code is not designed for the study of photodissociation processes, while MADWAVE3 is.

The use of hyperspherical coordinates in wave packet calculations [11, 12] is an interesting alternative to state-to-state dynamics. The main problem

with this approach is the difficulty of describing long-distance regions on each rearrangement channel, which requires very dense grids and basis in the hyperangles to describe the rovibrational states of diatomic fragments. This limits the use of this approach to relatively high energies.

Other related methods are the reactant-product decoupling (RPD) [13, 14, 15, 16], in which the wave packet is split into reactant and product channels, and its evolution is calculated separately in the most appropriate, while the flux between the different channels is exchanged using negative imaginary potentials. However, this method shows difficulties when the reaction presents wells giving rise to resonances, which are affected by the split description and the imaginary potential. This problem has recently been addressed [17] opening for new applications in the future.

In the following, we start introducing the theory behind the MADWAVE3 program in section 2, and its implementation in modules of the code. Next, in section 3 the installation procedures are described. In section 4, the system dependent programs needed to be applied to particular systems are described. Section 5, in Table 1 provides a comprehensive description of the various FORTRAN namelists and parameters involved in the code execution. Section 6 shows a benchmark example with steps to follow the execution. The parallelization efficiency of the code is presented in section 7, using the example of section 6. Finally, a summary is presented in the conclusions.

2. Theory

2.1. Coordinates and Hamiltonian

To describe the A+BC channel the Jacobi vectors $\mathbf{r}_{\alpha=A}$ (BC inter-nuclear vector) and $\mathbf{R}_{\alpha=A}$ (the vector joining BC center-of-mass to A atom) are defined. There are three sets of these coordinates, $\alpha = A, B$ and C defined in a cyclic way, each one adapted to describe the corresponding asymptotic solution as a simple product of monodimensional eigenfunctions for each rearrangement. Hereafter, the subscript α will be generally omitted (unless necessary) since the equations are formally equivalent for each set.

A body-fixed frame is used, in which the z-axis is parallel to the \mathbf{R} vector, and \mathbf{r} is in the x-z body-fixed frame. The body-fixed is obtained by a rotation, defined by the Euler angles (ϕ, θ, χ) , from the space-fixed frame, following the convention defined by Ref. [18]. Thus, in the body-fixed frame, the coordinates are divided into the three external Euler angles and the three internal coordinates (r, R, γ) , where r and R are the magnitudes of vectors

\mathbf{r} and \mathbf{R} , respectively, and $\gamma = \mathbf{r} \cdot \mathbf{R}/rR$ represents the angle between them. In these coordinates, the total wave packet is expressed as

$$\Psi_i^{JMp}(\mathbf{r}, \mathbf{R}; t) = \sum_{\Omega\Lambda} \frac{\Phi_{\Omega\Lambda}^{JMp}(r, R, \gamma; t)}{rR} W_{\Omega\Lambda}^{JMp}(\phi, \theta, \chi), \quad (1)$$

where i is a collection of quantum numbers that specify the initial state, and the angular-electronic functions are

$$W_{\Omega\Lambda}^{JMp}(\phi, \theta, \chi) = \sqrt{\frac{2J+1}{16\pi^2(1+\delta_{\Omega 0})}} \left[\begin{aligned} & D_{M\Omega}^{J*}(\phi, \theta, \chi) |\Lambda, \sigma\rangle \\ & + p\sigma(-1)^{J+\Omega} D_{M-\Omega}^{J*}(\phi, \theta, \chi) |-\Lambda, \sigma\rangle \end{aligned} \right] \quad (2)$$

with J, M, Ω being the total angular momentum, and its projections onto the space-fixed and body-fixed z-axis, respectively, p is the parity under inversion of spatial coordinates. $D_{M\Omega}^{J*}(\phi, \theta, \chi)$ are Wigner rotation matrices [18] and $|\Lambda, \sigma\rangle$ are electronic functions, with σ being the parity under reflection through the x-z body-fixed plane.

The $\Phi_{\Omega\Lambda}^{JMp}(r, R, \gamma; t)$ coefficients in Eq. (1) are represented in grids as

$$\Phi_{\Omega\Lambda}^{JMp}(r, R, \gamma; t) = \sum_{k,m,n} \langle r_k R_m \gamma_n | \Phi_{\Omega\Lambda}^{JMp}(t) \rangle, \quad (3)$$

using Gauss-Legendre quadrature points for γ , and equidistant points for the radial coordinates, r, R . The grids and basis set in reactants Jacobi coordinates are controlled through the **inputgridbase** namelist (see Table 1).

The triatomic Hamiltonian in Jacobi coordinates is written as

$$H = -\frac{\hbar^2}{2\mu} \left(\frac{2}{R} \frac{\partial}{\partial R} + \frac{\partial^2}{\partial R^2} \right) - \frac{\hbar^2}{2m} \left(\frac{2}{r} \frac{\partial}{\partial r} + \frac{\partial^2}{\partial r^2} \right) + \frac{\hat{\ell}^2}{2\mu R^2} + \frac{\hat{j}^2}{2mr^2} + H_e \quad (4)$$

with $\mu = m_A(m_B + m_C)/(m_A + m_B + m_C)$, $m = m_B m_C/(m_B + m_C)$ being the reduced masses, \hat{j} and $\hat{\ell}$ are the angular momentum operators associated to \mathbf{r} and \mathbf{R} . In the body-fixed frame $\hat{\ell}^2 = \hat{J}^2 + \hat{j}^2 - 2\hat{J} \cdot \hat{j}$. Finally, H_e is the electronic Hamiltonian represented in a diabatic electronic basis set $|\Lambda, \sigma\rangle$, so that $\langle \Lambda, \sigma | H_e | \Lambda', \sigma' \rangle = f(r, R, \gamma)$ are simple potential terms (with no kinetic couplings). Hereafter, it will be considered that asymptotically

(when $R \rightarrow \infty$) the electronic matrix is diagonal for one rearrangement (typically the one of the reactants) but not necessarily for the other two.

Insertion of Eq. (1) into the time-dependent Schrödinger equation using the Hamiltonian of Eq. (4), yields a set of first order differential equations for the $\langle r_k R_m \gamma_n | \Phi_{\Omega\Lambda}^{JMp}(t) \rangle$ coefficients

$$\begin{aligned}
i\hbar \frac{\partial \langle r_k R_m \gamma_n | \Phi_{\Omega\Lambda}^{JMp}(t) \rangle}{\partial t} = & \sum_{k'm'n'\Omega'\Lambda'} \left\{ \delta_{mm'} \delta_{nn'} \delta_{\Omega\Omega'} \delta_{\Lambda\Lambda'} \left\langle r_k \left| -\frac{\hbar^2}{2m} \frac{\partial^2}{\partial r^2} \right| r_{k'} \right\rangle \right. \\
& + \delta_{kk'} \delta_{nn'} \delta_{\Omega\Omega'} \delta_{\Lambda\Lambda'} \left\langle R_m \left| -\frac{\hbar^2}{2\mu} \frac{\partial^2}{\partial R^2} \right| R_{m'} \right\rangle \\
& + \delta_{kk'} \delta_{mm'} \delta_{\Omega\Omega'} \delta_{\Lambda\Lambda'} \left\langle \gamma_n \left| \frac{\hat{j}^2}{2mr_k^2} \right| \gamma_{n'} \right\rangle \\
& + \delta_{kk'} \delta_{mm'} \delta_{\Lambda\Lambda'} \left\langle \gamma_n \left| \frac{\langle W_{\Omega\Lambda}^{JMp} | \hat{\ell}^2 | W_{\Omega'\Lambda}^{JMp} \rangle}{2\mu R^2} \right| \gamma_{n'} \right\rangle \\
& \left. + \delta_{kk'} \delta_{mm'} \delta_{nn'} \delta_{\Omega\Omega'} \langle \Lambda, \sigma | H_e | \Lambda', \sigma' \rangle \right\} \langle r_{k'} R_{m'} \gamma_{n'} | \Phi_{\Omega'\Lambda'}^{JMp}(t) \rangle
\end{aligned} \tag{5}$$

The $\langle r_k R_m \gamma_n | \Phi_{\Omega\Lambda}^{JMp}(t) \rangle$ coefficients depend on 5 indexes: k, m, n, Ω, Λ , and each term of the Hamiltonian is non-diagonal in only one variable, except $\hat{\ell}^2$, which is non-diagonal in two: n and Ω . However, the Coriolis term only couples Ω values with $\Delta\Omega = 0, \pm 1$, *i.e.* it is a tridiagonal term. All this allows to asses:

1. Each term of the Hamiltonian is applied sequentially, which means that the multiplication of a monodimensional matrix and a vector, within the 5 dimensional vector of coefficients. This implies 6 nested loops.
2. The two radial terms are further accelerated by applying a Fourier transform method using the FFTW3 library¹ (the current version is not ready for the version included in MKL library). In particular, we use the real sine transform to impose the proper regular boundary conditions at $R = 0$ [19, 20], and to keep the wave packet propagation real, as will be described below.

¹The FFTW3 library is not thread-safe and for some compilers it may result in wrong executions. Please be aware of this problem and compare with the executions compiled with the **-fno-omp** flag in gfortran compiler.

3. The two angular kinetic terms, \hat{j}^2 and $\hat{\ell}^2$, are applied following a transformation from a discrete variable representation (DVR) to a finite basis set (FBR), in which the matrix elements are analytical, as explained in Ref. [1].
4. The $\hat{\ell}^2$ term, presenting the extra difficulty of being tridiagonal in Ω is easily parallelized in this index, thus minimizing the communication among processors [1].
5. The electronic Hamiltonian (hereafter potential term), is diagonal in the internal coordinates. This term can reach very high values, so it is generally advisable to limit it to a finite maximum value, out of the physically relevant interval. This approach also significantly reduces memory usage, as the entire configuration space can be limited to only the accessible region, known as L-shaped grids [21]. This reduction is done before running the wave packet calculations, in the preparation of the potential matrix elements, read by the MADWAVE3 program.

The action of the Hamiltonian on the wave packet is evaluated in module **mod_Hphi_01y2.f**. The potential is read from the directory **../pot**, which is generated in the preparation stage with the system dependent code **pot.out** (see section 4) using the module **mod_pot_01y2.f** on the grid defined above, and the **vcutmax_eV** in **namelist inputpotmass** where also the atomic masses are provided. The grid and basis sets are defined in modules **mod_gridYpara_01y2.f** and **mod_baseYfunciones_01y2.f**

2.2. Propagation and absorption

The propagation is performed with a modified Chebyshev propagator, proposed by Mandelshtam and Taylor [22] as a modification including absorption of the original Chebyshev propagator by Tal-Ezer and Kosloff [23]. Several alternative but equivalent forms of these propagators have been proposed [24, 25, 26, 27, 28]. Basically, the Chebyshev components of the wave packet are obtained iteratively as

$$\begin{aligned}
 \Psi(k=0) &= \Psi(t=0) \\
 \Psi(k=1) &= e^{-\varphi} \hat{H}_s \Psi(k=0) \\
 \Psi(k+1) &= e^{-\varphi} \left\{ 2\hat{H}_s \Psi(k) - e^{-\varphi} \Psi(k-1) \right\},
 \end{aligned} \tag{6}$$

where $\hat{H}_s = (\hat{H} - E_0) / \Delta E$ is the scaled Hamiltonian, with $E_0 = (E_{max} + E_{min})/2$, $\Delta E = (E_{max} - E_{min})/2$ and $E_s = (E - E_0) / \Delta E$, E_{max} and E_{min}

being the minimum and maximum energy values of the Hamiltonian of the system represented in the grid/basis used in the propagation. In Eq. (6), the initial Chebyshev component is defined as the initial wave packet, and $e^{-\varphi}$ is a real damping function, introduced to avoid transmission and reflection of the wave packet in finite grids when the edges are reached. To first order, the φ function can be related to a purely imaginary potential, V_I ($V_I \approx i\varphi$), fulfilling

$$\varphi(x) = \begin{cases} 0 & \text{for } x < x_I \\ A_x(x - x_I)^{n_I} & \text{for } x > x_I \end{cases}, \quad (7)$$

with $x \equiv r$ or R . The absorption parameters n_I, x_I (R_I, r_I) and A_x (A_R, A_r) need to be optimized to minimize the absorption effects on the wave packet in the interaction region [29]. The transmission through the absorption region, *i.e.* from x_I to x_{max} , can be strongly reduced by increasing either A_x or x_{max} . The major problem, however, is the reduction of the reflection back to the interaction region [29]. This is the case when low final translation energies between reactants or products play an important role, in the opening of new channels. When the de Broglie wavelength, λ_{dB} , increases, the absorption region should be augmented to an integer factor of λ_{dB} , but this may lead in some cases to use prohibitively large grids.

With these definitions, the Chebyshev components stay real if the initial wave packet is real, what allows to considerably reduce the memory requirements in computational implementations. Also, working in the Chebyshev domain allows to reduce the number of iterations required to get magnitudes defined either in the time- or the energy-domain. This is achieved by transforming either to a time-dependent wave packet or to an energy-dependent wave function using the expressions

$$\begin{aligned} \Psi(t) &= \sum_{k=0}^{\infty} f_k(\hat{H}_s, t) \Psi(k) \\ \Psi(E) &= \frac{1}{a_0(E)} \sum_{k=0}^{\infty} c_k(\hat{H}_s, E) \Psi(k) \end{aligned} \quad (8)$$

where $a_0(E)$ is defined below, and

$$\begin{aligned} f_k(\hat{H}_s, t) &= (2 - \delta_{k0}) e^{-iE_0 t/\hbar} (-i)^k J_k(t\Delta E/\hbar) \\ c_k(\hat{H}_s, E) &= (2 - \delta_{k0}) \frac{\hbar \exp[-ik \arccos E_s]}{\sqrt{\Delta E^2 - (E - E_0)^2}} \end{aligned} \quad (9)$$

with J_k being Bessel functions of the first kind.

The Chebyshev propagation is performed in the main program **main_madwave3.f** using the input parameters defined in **namelist inputtime** (in input.dat). The absorption is defined in module **mod_absorcion_01y2.f** using the parameters provided by the user in the **namelist inputabsorcion** (in input.dat).

2.3. Initial wave packet

Two cases will be considered: one for collisions on the reactants channel, and the other for photodissociation in the interaction region. These are defined separately below. The process is defined by the variable **iphoto** = 0 or 1 in the **namelist inputprocess** (in input.dat) and is read in module **mod_gridYpara_01y2.f**

2.3.1. Initial wave packet in collisions

The initial wave packet for collisions is defined for a particular rovibrational state of the reactants, given by the quantum number $\alpha = J, p, \Lambda_0, v_0, j_0, \Omega_0$, as

$$\Psi^\alpha(t=0) = W_{\Omega_0\Lambda_0}^{JMp} \chi_{v_0j_0}(r) Y_{j_0\Omega_0}(\gamma) g(R), \quad (10)$$

where $\chi_{vj}(r)$ are the vibrational eigenfunctions of the diatomic reactant, $Y_{j\Omega}(\gamma)$ are normalized associated Legendre functions and $g(R)$ is a real function obtained as a linear superposition of incoming and outgoing plane waves of the form [28]:

$$g(R) = \frac{e^{-(R-R_0)^2/2\Gamma^2}}{2[\pi\Gamma^2]^{1/4}} [e^{-ik_0R} + e^{ik_0R}]. \quad (11)$$

As mentioned in Ref. [28] only the incoming half of the initial wave packet yields to products. Therefore, the evaluation of the reaction probabilities only requires the initial flux corresponding to the incoming waves, *i.e.*, at a given energy, only a half of the flux is taken into account.

The incoming flux in the initial state of the reactants, provided that the wave packet at $t = 0$ is located at a sufficiently long distance where the potential is constant, is defined as

$$a_0(E) = \frac{1}{2i} \sqrt{\frac{\mu}{2\pi\hbar^2 K_0(E)}} \int dR e^{iK_0(E)R} g(R) \quad (12)$$

with $K_0(E) = \sqrt{2\mu(E - E_{v_0j_0})/\hbar^2}$, with $E_{v_0j_0}$ being the energy of the initial rovibrational eigenstate of the BC reagent.

The initial wave packet in collisions is defined in the module **mod_colini_01y2.f** using the data in **namelist inputcol**.

2.3.2. Initial wave packet in photodissociation

In the framework of first order perturbation theory for the photodissociation of an initial bound state, $\Psi_{Xi}^{J_i M_i p_i}$, in electronic state X and vibrorotational state i , to a final electronic state Λ in a particular rotational state J , the initial wave packet is built as [30]

$$\left| \Psi_{\Lambda}^{JM p \leftarrow J_i M_i p_i}(t=0) \right\rangle = \sum_{\Omega} \left| W_{\Omega_{\Lambda}}^{JM p} \right\rangle \left\langle W_{\Omega_{\Lambda}}^{JM p} | \mathbf{d} \cdot \mathbf{e} | \Psi_{Xi}^{J_i M_i p_i} \right\rangle, \quad (13)$$

where \mathbf{d} are the matrix elements of the electric dipole moment between the ground X and the excited Λ electronic states, which depends on the internal coordinates r, R, γ . Its components are expressed in the molecular body-fixed frame, while the polarization vector, \mathbf{e} , of the incident photon defines the space fixed frame, so that the transition operator is written as

$$\mathbf{d} \cdot \mathbf{e} = \sum_{pq} (-1)^p (\mathbf{e})_{-p} D_{pq}^{1*}(\phi, \theta, \chi) d_q(r, R, \gamma), \quad (14)$$

where $p = 0$ for linearly polarized light (with the z space-fixed frame along the polarization vector of the photon) or $p = \pm 1$ for left/right circularly polarized (with the z space-fixed axis along the propagation of the incident photon).

The energy content of the initial wave packet is not known in this case, and needs to be evaluated along the propagation. This is done by doing the Fourier transform

$$a_0(E) = \frac{1}{2\pi\hbar} \int_{-\infty}^{\infty} dt e^{iEt\hbar} \left\langle \Psi_{\Lambda}^{JM p \leftarrow J_i M_i p_i}(t=0) \left| \Psi_{\Lambda}^{JM p \leftarrow J_i M_i p_i}(t) \right\rangle \quad (15)$$

which using Eqs. (9), in terms of the Chebyshev components becomes

$$a_0(E) = \frac{1}{\pi} \sum_{k=0}^{\infty} (2 - \delta_{k0}) \frac{\cos(-k \arccos E_s)}{\Delta E \sqrt{1 - E_s^2}} \left\langle \Psi_{\Lambda}^{JM p \leftarrow J_i M_i p_i}(k=0) \left| \Psi_{\Lambda}^{JM p \leftarrow J_i M_i p_i}(k) \right\rangle \quad (16)$$

The initial wave packet for photodissociation processes is defined in module **mod_photoini_01y2.f**, using the data defined in **namelist inputbnd**.

It reads system dependent data: the initial bound state in directory `../bnd` and the transition dipole moment in directory `../dip`. The initial bound state can be calculated using the `main_boundlanz.f` program (also in this version with compiled name `bound.out`) which calculates the bound states using an iterative non-orthogonal Lanczos method [31] in a grid, and the matrix elements are evaluated as described above for the wave packet. The transition dipole moment is evaluated in the preparation stage, by the main program `pot.out`, calling the routine `dipele.f` which should be supplied for each system as described below.

2.4. Analysis of final states

When the final state distribution is not needed, and only the reaction probability versus energy is required, the method of the total flux is probably the best choice [32, 33, 34, 35]. The total reaction probability then becomes

$$\begin{aligned}
 P^{Jp\alpha}(E) &= \sum_{\beta v' j' \Omega'} \left| S_{v_0 j_0 \Omega_0, \beta v' j' \Omega'}^{Jp}(E) \right|^2 \\
 &= \frac{K_0(E)}{\mu m} \sum_{\Omega} \sum_{\Lambda} \int dR \sin \gamma d\gamma \text{Im} \left[\Psi^{Jp\alpha+*}(E) \frac{\partial \Psi^{Jp\alpha+*}(E)}{\partial r} \Big|_{r^*} \right],
 \end{aligned} \tag{17}$$

where $\Psi^{Jp\alpha+*}(E)$ is given in Eq. (6) and r^* is a sufficiently long BC inter-nuclear distance. Since positive outgoing and negative incoming flux are accounted for, the total reaction probability is independent of the particular value of r^* [32]. Thus r^* does not need to be in the asymptotic region; it is typically positioned just beyond the saddle point for the reaction, where the flux converges more quickly.

The total flux is evaluated in module `mod_flux_01y2.f` using the parameters defined in `namelist inputflux` (in `input.dat`).

In Eq. (17), the summation runs over the products rearrangements, $\beta = B, C$, and all final rovibrational states of the products, v', j', Ω' , and $S_{v_0 j_0 \Omega_0 \Lambda_0, \beta v' j' \Omega'}^{Jp}(E)$ are matrix elements of the scattering S-matrix. The flux for individual final states is determined by the square of the corresponding S-matrix element, $\left| S_{v_0 j_0 \Omega_0 \Lambda_0, \beta v' j' \Omega'}^{Jp}(E) \right|^2$ and need to be computed at sufficiently long distances so that the interaction potential between A + BC, B+CA or C+AB fragments is zero.

We will define the final states of the products as

$$\varphi_{\beta,v',j',\Omega'} = \sum_{\Lambda'} W_{\Omega'\Lambda'}^{Jp}(\phi', \theta', \chi') \frac{Y_{j'\Omega'}(\gamma', 0) \chi_{v'j'}(r')}{r' R'}, \quad (18)$$

which are eigenstates of the products at long R' values, where it is assumed that the diabatic electronic states are not coupled on the reactants while for products the electronic states may be coupled. Therefore, the rovibrational states of the products are in general calculated in a coupled set of electronic states [36], and the quantum number v' is then used to denote the vibrational and electronic states.

Defining the projection coefficient at Chebyshev iteration k as

$$C_{v'j'\Omega'\beta}(k) = \int dV_{\beta} \delta(R' - R'_{\infty}) \left\langle \varphi_{\beta,v',j',\Omega'} \left| \Psi^{Jp}(k) \right. \right\rangle, \quad (19)$$

the S -matrix elements are defined as [37, 28, 2]

$$S_{v_0j_0\Omega_0,\beta v',j'\Omega'}^{Jp}(E) = -i \sqrt{\frac{2K'}{\pi\mu'}} \frac{e^{-iK'R'}}{a_0(E)} \sum_k c_k(\hat{H}_s, E) C_{v'j'\Omega'\beta}(k). \quad (20)$$

with $K'(E) = \sqrt{2\mu'(E - E_{v'j'\Omega'})/\hbar^2}$ with μ' and $E_{v'j'\Omega'}$ being the reduced mass and diatomic eigenvalues for products.

The problem to evaluate the coefficients in Eq. (19) is that in general the two wave functions are written in different Jacobi coordinates, one corresponding to reactants and the other to products.

The use of either reactants or products Jacobi coordinates, requires the use of large grids to describe at the same time the two asymptotic regions. One alternative, when the reaction is direct and does not present any wells, is the use of the so called Reactant-Product Decoupling (RPD) method [14, 15, 16, 38, 13]. In this method, the wave packet is split in reactant and product channels, and its evolution is calculated separately in the best suited coordinates. The flux between different channels is exchanged using Negative Imaginary Potentials [16, 13]. Transforming the coordinates is non-trivial, as a straightforward approach would nearly double the number of coordinate indices required (five in this case: r, R, γ, Ω , and Λ). To illustrate the computational cost of this transformation, applying the Hamiltonian to the wave packet involves $5 + 1$ nested loops.

In a more general case, to get the state-to-state reaction probabilities only one set of Jacobi coordinates is chosen. In these cases, the internal grids have to be larger to cover all the rearrangement channels. There are two alternatives:

1. Products coordinates based (PCB) method: the initial wave packet, written as a product of monodimensional functions in reactants coordinate, is transformed to products. In this case the overlap required in Eq. (19) can be done directly.
2. Reactants coordinates based (RCB) method: in which the wave packet at each Chebyshev iteration has to be transformed. To do so, a sequential transformation, passing through intermediate coordinates, is done as it has been proposed [2].

The choice between PCB and RCB depends on the masses involved in the mass combination as discussed in detail in Ref. [2]. Thus for heavy-light + heavy' \rightarrow heavy-heavy' + light the RCB method is very effective. In the case of heavy-light+heavy' \rightarrow heavy +light-heavy' case PCB is better. In the intermediate case, the choice is flexible, with the symmetry of identical atom permutations playing an important role.

The parameter **iproduct** in the **inputproduct** namelist controls whether only the total flux is computed (= 0), computes the state-to-state probabilities using products Jacobi coordinates (= 1) or computes the state-to-state probabilities using reactant Jacobi coordinates (= 2).

2.5. Cross sections

The state-to-state cross sections for reactive and inelastic collisions are obtained in the usual partial wave summation as

$$\sigma_{v_0 j_0 \Lambda_0, \beta v', j'}(E) = \frac{\pi}{K_0(E)^2 (2j_0 + 1)} \mathcal{C}_{v_0 j_0 \Lambda_0, \beta v', j'}(E) \quad (21)$$

where the cumulative probability, $\mathcal{C}_{v_0 j_0 \Lambda_0, \beta v', j'}(E)$ is defined as

$$\mathcal{C}_{v_0 j_0 \Lambda_0, \beta v', j'}(E) = \sum_J \sum_p \sum_{\Omega} \sum_{\Omega_0} (2J + 1) \left| S_{v_0 j_0 \Omega_0, \beta v', j' \Omega'}^{Jp}(E) \right|^2. \quad (22)$$

This expression needs to have the individual S-matrix elements for all J , p and Ω_0 calculated previously. Following the J-shifting approach [39], the individual probabilities are shifted up as J increases.

	EXAMPLES	Examples for different applications
	SRC	Source code files
	.gitignore	
	README.md	Minimal usage comments

To compile the code navigate to the **BIN** directory and run either the Makefile or bash script **colmad3.sh** to compile the **mad3.out** code or **bnd3.out** devoted to calculation of bound states. Several other auxiliary codes are compiled in this step, which will be indicated latter. In order to compile all these codes with the Makefile type “make main aux”. The compilation requires two libraries: MPI (we use OpenMPI) and FFTW3 (the implementation in MKL does not work with the present set of parameters). The code has been tested with gfortran and Intel Fortran Compiler compilers. In new versions of gfortran, the use of **include** “**mpif.h**” is deprecated, and without changing the codes this problem can be avoided by including the flags in the compilation (using Makefile or colmad3.sh): **FCFLAGS=“-DUSE_MPIF -fallow-invalid-boz -fallow-argument-mismatch”**.

The FFTW3 library is not thread-safe. For this reason the use of OpenMP is not direct, and a procedure has been implemented to solve this problem. Therefore, the use of OpenMP should be checked. Once this is done, the options to use OpenMP (for example, “-fopenmp” when using gfortran) have to be added to the Makefile or colmad3.sh procedures.

In the directory **EXAMPLES** some examples are provided, discussed below, which use some potential and electric dipole moments in directory **PES**.

The two main programs, **mad3.out** and **bndgrid.out**, use some system dependent data that must be prepared in a preparation stage: the potential, in directory **pot** and the matrix dipole moments, in directory **dip**. In addition, the rovibrational states of diatomic fragments for reactants and products are calculated and kept in directory **func**. The three directories must be created and empty before execution of program **pot.out**, which must be compiled with the Makefile or script **colpot.sh** using system dependent subroutines provided by the user, as described below.

4. System dependent programs provided by the user

The user must provide three routines for the **pot.out** program to generate the data required to run MADWAVE3: **setxabcotele**: This routine supplies

information about the electronic states and initializes the data needed to call the potential in the second routine, **potelebond**. In the case of photodissociation, also the transition dipole moments need to be provided in the **dipele** routine. The arguments of these three routines are explained below:

```

subroutine setxhcpotele(iomdiat,iomatom,sigdiat,sigatom, &
                        nelec,nelecmax)
  ! Initialize variables of the user provided PES.
  ! iomdiat: Projection of the orbital electronic
  !           angular momentum (Lambda) for each of
  !           the nelec states considered (or Omega
  !           in Hund's case c)
  ! iomatom: Similar to iomdiat but for the atom.
  ! sigdiat: Parity for the reflection of electronic
  !           wave function through the xz-body fixed
  !           fram of the diatomic fragment.
  ! sigatom: Similar to sigdiat but for the atom.
  ! nelec: Number of electronic states considered.
  ! nelecmax: Total number of electronic states in the
  !           PES, usually equal to nelec.
  implicit none
  integer, intent(in) :: nelec, nelecmax
  integer, intent(out) :: iomdiat(nelecmax)
                        iomatom(nelecmax)
                        sigdiat(nelecmax)
                        sigatom(nelecmax)

  ! Set values
  ! If required, execute the PES initialization
end subroutine setxhcpotele

```

```

subroutine potelebond(r10, r02, costet, potmat, nelec, &
                      nelecmax)
  ! Compute the potential energy matrix.
  ! r10, r02: Diatomic internuclear distances for the
  !           AB and BC fragments. In Bohr.
  !           When iprod = 1, AB+C are products.
  ! costet: Cosine of the angle formed by r01 and r02.
  ! potmat: Potential energy matrix in the diabatic

```



```

!           representation. In Hartree.
! nelec: Number of electronic states considered.
! nelecmax: Total number of electronic states in the
!           PES, usually equal to nelec.
implicit none
integer, intent(in) :: nelec, nelecmax
real(8), intent(in) :: r10, r02, costet
real(8), intent(out) :: potmat(nelecmax, nelecmax)

! Fill potmat with a user defined PES
end subroutine potelebond

```

```

subroutine dipele(rp, Rg, cgam, dx, dy, dz, nelec, nelecmax)
! Compute the electronic transition dipole moments.
! rp, Rg: Distances in Jacobi coordinates.
!           Small and big rs.
!           In Bohr.
! cgam: Cosine of the angle between r and R.
! dx, dy, dz: Electronic transition moments from a single
!             initial electronic state to the nelec
!             electronic states considered, for the
!             x, y, z components of the Jacobi
!             body-fixed frame.
!             In atomic units, NOT Debye.
! nelec: Number of electronic states considered.
! nelecmax: Total number of electronic states in the
!           PES, usually equal to nelec.
implicit none
integer, intent(in) :: nelec, nelecmax
real(8), intent(in) :: rp, Rg, cgam
real(8), intent(out) :: dx(nelec), dy(nelec), dz(nelec)

! Fill dx, dy, dz
end subroutine dipele

```

To execute the program **pot.out**, the directories **pot**, **func** and **dip** (if needed) must be in the parent directory with respect to the working directory (i.e. as **../pot**, etc)

In **potebond** the input variables r_{10} , r_{02} , costet determine the geometry of the triatomic system. Often, the potentials developed for triatomic systems are expressed as:

1. Internuclear distances r_{10} , r_{12} , r_{02} : in this case the missing r_{12} distance is directly obtained as

$$r_{12} = \sqrt{r_{10}^2 + r_{02}^2 - 2r_{10}r_{02}\cos\gamma} \quad (25)$$

where $\cos\gamma$ is in the costet variable.

2. In Cartesian coordinates for the three atoms $x_0, y_0, z_0, x_1, y_1, z_1, x_2, y_2, z_2$: Assuming the three atoms in the x-z plane, with atom 0 at the origin and atom 1 along the z-axis, the Cartesian coordinates are then obtained as

$$z_1 = r_{10}, \quad z_2 = r_{02}\cos(\gamma) \quad x_2 = r_{02}\sin(\gamma), \quad (26)$$

after initializing all Cartesian coordinates to zero.

Many triatomic systems have been studied, with many different mass combinations, in collisions such as $\text{Li}+\text{HF}\rightarrow\text{LiF}+\text{H}$ [35, 43], $\text{O}+\text{HF}\rightarrow\text{F}+\text{OH}$ [40, 41], C^++H_2 [44], S^++H_2 [45, 46], $\text{Ca}+\text{HCl}$ [47], $\text{H}+\text{H}_2^+$ [48], H^++H_2 [20], $\text{F}+\text{DCI}$ [49], $\text{N}+\text{OH}$ [50], H^++LiH [42], and photoinitiated processes in LiHF [30, 51], ArI_2 [52], HCN [53, 54], OHF^- [55, 56], etc.

The program **pot.out** calculates the bound states of the reactant and products diatomic fragments. The diatomic potentials of the reactants (01) and products (02) are printed in the files **potr.eEE** and **potdia-prod02.dat**, where (EE denotes the electronic state). The examination of these potentials, together with the eigenvalues (in `salpot.000`) and eigenfunctions (in `wv01-ielecEE-j00.dat` and `wv02-vVVj0.dat`) of 01 and 02 diatomic fragments provides a simple way to check the implementation of a new PES. Also, for $J=0$ and setting `iwrt_pot=1` (in the namelist `INPUTWRITE` described below), the execution of program **mad3.out** prints the PES in the files **potr1r2.eEE.FF**, in the grid of points defined in `inputwrite`, as described below. Note, that this potential is shifted so that the energy of the reactant level determined by `IELECREF,NVREF,JREF,IOMREF` has zero energy.

In the case of several coupled electronic states, a diabatic representation is assumed[57, 58, 59, 60, 61, 62, 56, 63, 64]. The diabatic representation is built by a unitary transformation from the usual adiabatic representation. It allows the inclusion of the coupling among different electronic states through

a slowly varying potential term. The singularity of non-adiabatic couplings at conical intersections is avoided in the diabatic representation, thus presenting computational advantages. Diabatic representations are not unique and cannot remove all the non-adiabatic terms in polyatomic systems [59], but they allow to regularize the singularities at conical intersections [61]. There is no standard method to generate the diabatic states, specially beyond two electronic states and there is a pleiad of methods [57, 58, 59, 60, 61, 62, 56, 63, 64].

In general, it is assumed that the diabatic states correlate to the adiabatic ones at long distances. In such situation, there is no coupling among different electronic states, and the rovibrational states of the diatomic fragments in each rearrangement could be calculated independently in each electronic state. When dealing with reactions, this is not always the case. For example, the diabatic states of H_3^+ can be formed in a simple basis in which each electronic state corresponds to a charge in a single H atom [65]. This is true when studying $\text{H}_2 + \text{H}^+$. However, for $\text{H}_2^+ + \text{H}$ this is not the case, and a choice has to be made in which rearrangement channel the diabatic and adiabatic representations coincide at long distances, as it was done recently in the study of non-adiabatic transition in $\text{H}_2^+ + \text{H}$ reactive collisions [36]. For this reason, in MADWAVE3 the rovibrational states for the O2 products are calculated in the full manifold of electronic states, and in `wv02-vVVj0.dat` files each vibrational state VV is represented as a linear superposition in the different electronic states.

5. Input data

The rest of the input data is provided in different namelists in the file **input.dat** that must be in the working directory. Below the parameters of the different namelists are listed and briefly explained in Table 1.

Table 1: Brief description of the data included in each namelist in **input.dat**. Distances in Å, energies in eV. Variables with initial letter starting k-q are integer, otherwise they are real*8. Default values are given in parenthesis

inputgridbase

Continued on next page

Table 1: Brief description of the data included in each namelist in **input.dat**. Distances in Å, energies in eV. Variables with initial letter starting k-q are integer, otherwise they are real*8. Default values are given in parenthesis (Continued)

npun1,rmis1,rfin1	r no. of points in the interval [rmis1, rfin1]
npun2,rmis2,rfin2	R no. of points in the interval [rmis2, rfin2]
nangu	no. of Gauss Legendre quadrature points for γ
Jtot	total angular momentum, J
iparity	total inversion parity, p
jini,jmax	first and last reactants BC angular momentum for flux evaluation
inc	=1, 2 for hetero or homo nuclear BC molecules
j0	initial value of j when inc=2
neleemax	no. of electronic states
iomini(0) , iommax	Ω values in the expansion of wvp, Eq. (1)
nvini,nvmax	first and last vibrational levels of BC reactants
nvref,jref,iomref,ielecref	$v_0, j_0, \Omega_0, \Lambda_0$ reactants quantum numbers, Eq. (10). Its energy is taken as the zero of energy.
inputprod	
iproduct (0)	= 0 only total flux = 1 products coordinates for state-to-state prob. for levels defined by jini,jmax,nvini,nvmax = 2 using reactant coordinates for state-to-state prob. products levels defined below

Continued on next page

Table 1: Brief description of the data included in each namelist in **input.dat**. Distances in Å, energies in eV. Variables with initial letter starting k-q are integer, otherwise they are real*8. Default values are given in parenthesis (Continued)

nviniprod,nvmaxprod	first and last vibrational states of products, v' in Eq. (18)
jiniiprod,jmaxiprod	first and last rotational states of products, j' in Eq. (18)
iomminprod(0),iommaxprod(0)	initial and final Ω' of products
Rbalinprod	R'_∞ at which the flux on products is done, Eq. (19)
n2prod0(1),n2prod1(npun2)	initial and final grid points to represent. Vib. functions in intermediate representation (to save memory and reduce coordinate transformation time).
inputprocess	
iphoto	= 0 collision, =1 photodissociation
inputtime	
ntimes	number of Chebyshev iterations, k , per loop, Eq. (6)
nloop	number of loops
kminelastic	initial k at which the elastic flux is evaluated
inputflux	
r1flux_ang	r^* value at which flux is evaluated, (=absr1-1) Eq. (17)
netot	number of energies at which flux is evaluated
ekinmin_eV	minimum energy for flux evaluation
ekinmax_eV	maximum energy for flux evaluation

Continued on next page

Table 1: Brief description of the data included in each namelist in **input.dat**. Distances in Å, energies in eV. Variables with initial letter starting k-q are integer, otherwise they are real*8. Default values are given in parenthesis (Continued)

ncontfile	=1 for long propagations to restart calculations. Restarting files are written at the end of each loop
inputwrite	
iwrt_pot(0)	if 1 writes the potential in files potr1r2.eX.Y for r_k, R_m, γ_n $k=1,1+n1plot,1+2 n1plot, \dots, npun1$ $m= 1,1+n2plot, 1+2 n2plot,\dots, npun2$ $n=1,1+nangplot, 1+2 nangplot, \dots, nangu$
iwrt_wvp	if =1 write the wave packet for r_k, R_m, γ_n at each loop
iwrt_reac_distri	= 0 don't write reactants distribution (except iprod=1) = 1 writes reactants probabilities in files the file is overwritten at each loop = 2 writes overlap of Eq. (19) to re-process the final distribution (needed when iconfile=1)
n1plot,n2plot,nangplot	defined for iwrt_pot
inputpotmass	
system	character*20 "name of system"
xm1,xm0,xm2	masses in amu of atoms 01 + 2 → 1 +02
VcutmaxeV	maximum values in eV of potential energy
radcutmaxeV	maximum values in eV of radial kinetic energy

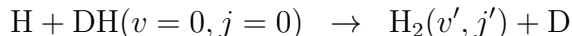
Continued on next page

Table 1: Brief description of the data included in each namelist in **input.dat**. Distances in Å, energies in eV. Variables with initial letter starting k-q are integer, otherwise they are real*8. Default values are given in parenthesis (Continued)

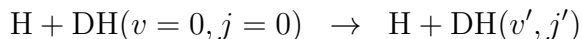
rotcutmaxeV	maximum values in eV of rotational energy
R2inf_radial_functions	distance R to calculate reactant vibrational states (100 bohr)
R1inf_radial_functions	distance R to calculate products vibrational states (100 bohr)
inputbnd	
Jtotini,iparini	total angular momentum J_i and parity p_i of initial bound state
nvbound	vibrational state to read, as generated by bndgrid.out
nprocbnd	processors(files) used to calculate initial bound state
maxbnddim	maximum size to the vectors used for bound state
igrdbnd	must be 1 if using bndgrid.out
inputcol	
Rcolini_ang	R_0 center of initial Gaussian (in Å) for collisions, Eq. (11)
ecol_eV	mean collision energy (eV) of initial Gaussian
deltaE_eV	energy width (in eV) of initial Gaussian.
inputabsorcion	
absr1,absalp1,n1expo(2)	r_I (Å), A_r and n_i for r in Eq. (7)
absr2,absalp2,n2expo(2)	R_I (Å), A_R and n_i for R in Eq. (7)

6. Examples and Output

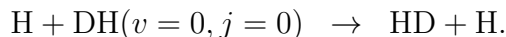
The prototype state-to-state reactive collision



is studied here, also considering the inelastic process,



For the exchange process only the total reaction probability and total cross section is calculated:



In the following we present a shorter version of the example which can be found in the `EXAMPLES` folder of the `MADWAVE3` repository.

6.1. Preparatory step

The first step is to compute the PES and reactants (and products) eigenfunctions. For that, we must specify information about the grid used to represent the PES, the masses the atoms and whether the states of the products should be computed. Here we explain some of the parameters that should be set in the `input.dat` file.

```
&INPUTGRIDBASE
! 256 grid points from 0.1 to 20 A
NPUN1= 256, RMIS1= 0.1d0, RFIN1= 20.d0, NPUN1MIN= 64,

! 256 points from 1e-3 to 20 A
NPUN2= 256, RMIS2= 0.001d0, RFIN2= 20.d0,
NANGU= 140 ! 140 angular points
NELECMAX= 1, ! 1 electronic state
JTOT= 0, IPARITY= 1
IOMMIN= 0, IOMMAX= 0,
JO= 0, INC= 1

! j=0 to j=39 for reactant's rotational states
JINI= 0, JMAX= 39,
```



```

! v=0 to v=5 for reactant's vibrational states
NVINI= 0, NVMAX= 5,

NVREF= 0, JREF= 0, IOMREF= 0, IELECREF= 1,
/

```

```

&inputpotmass
!-----> masses(in amu) and potential(in eV) cut data
system='H+DH'
xm0=2.014101779d0 ! mass of atom 0
xm1=1.007825035d0 ! mass of atom 1
xm2=1.007825035d0 ! mass of atom 2
VcutmaxeV=2.5d0 ! maximum potential energy
radcutmaxeV=2.5d0
rotcutmaxeV=5.d0
/

```

```

&inputprod
iprod=2 ! =0 no products state distribution,
        ! =1 using products Jacobi coordinates,
        ! =2 using reactants Jacobi coordinates,
        !transforming to products to extract s2s properties

! v=0 to v=5 for product's vibrational states
nviniprod=0,nvmaxprod=5

! j=0 to j=20 for product's rotational states
jiniprod=0, jmaxprod=20

iomminprod=0! , iommaxprod=0 ! Jtot
Rbalinprod=6.d0
n2prod1=256 !npun2/2
/

```

In this example we employ an in-house PES provided in the MADWAVE3 repository which reproduces very well the PES by Pendergast (BKMP2). This potential presents a barrier to reactions of ≈ 0.25 eV, and the study

will be performed up to 1.5 eV above the $\text{H} + \text{DH}(v = 0, j = 0)$ initial state, which determines the zero of energy. Final states up to $v=5$ and $j=40$ states will be considered for reactants and products. Also, potential will be cut to $\text{vcutmax_eV} = 2.5$ eV.

Our H_3 PES is invoked through the VH3 subroutine, which receives as input the three interatomic distances.

```

subroutine VH3(RAB,RBC,RAC,VTOT,DVTOT,ID)
  ! RAB, RBC, RAC: interatomic distances
  ! VTOT: Electronic energy
  ! DVTOT: Derivatives of the energy w.r.t. distances
  !         (not implemented)
  ! ID: status of computation
  use H3pot ! module with actual PES.
  implicit none
  real(8), intent(in) :: RAB, RBC, RAC
  real(8), intent(out) :: VTOT
  real(8), dimension(3), intent(out) :: DVTOT
  integer, intent(out) :: ID
  ! Computation...
end subroutine VH3

```

In this particular case, the routines which interface the PES with MAD-WAVE3 (setxabcotele and potelebond) are defined in the pothead.f file:

```

subroutine setxabcotele(iomdiat,iomatom,sigdiat,sigatom
&                      ,nelec,nelecmax)
  implicit real*8(a-h,o-z)
  dimension iomdiat(nelecmax),iomatom(nelecmax)
  dimension sigdiat(nelecmax),sigatom(nelecmax)

  write(6,*)'Potential setting message'

  ! Check that only one electronic state is being used.
  if(nelecmax.ne.1)then
    write(6,
&      '(" This PES is prepared for a single state ")')
    stop

```

```

endif
nelec=1
iomdiat(1)=0
iomatom(1)=0
sigdiat(1)=+1
sigatom(1)=+1
return
end setxabcotele

subroutine potelebond(r1,r2,costet,potmat,nelec,nelecmax)
  use H3_pot
  implicit real*8(a-h,o-z)
  dimension potmat(nelecmax,nelecmax)
  dimension der(3)
  rref=1.4d0
  rasi=100.d0
  call VH3(rasi,rasi,rref,pot,der)
  vref=pot

  ! Compute the third distance.
  r3=r1*r1+r2*r2-2.d0*r1*r2*costet
  r3=dsqrt(r3)
  if(r1.lt.0.25d0)r1=0.25d0
  if(r2.lt.0.25d0)r2=0.25d0
  if(r3.lt.0.25d0)r3=0.25d0
  call VH3(r3,r2,r1,pot,der)
  potmat(1,1)=pot-vref
  return
end potelebond

```

The **pot.out** code can be compiled with the Makefile provided in the package.

The empty directories **pot** and **func** are created prior to the execution of **pot.out** code, which will compute the PES in the selected grid and the reactant's and product's wavefunctions.

6.2. Reaction probabilities at $J = 0$

Usually, the calculations for $J = 0$ are first converged prior to calculating the remaining J 's. This requires to check the parameters of the grids until full convergence of the different energy-resolve state-to-state probabilities is reached. This of course implies to check how these quantities converge with the number of Chebyshev iterations. The parameters of the calculations are printed in files **sal.XYZ**, where XYZ runs from 0 to the number of processors minus one. Once the propagation starts, the norm of the Chebyshev wave packet at iteration k , $\Psi(k)$, is printed only in sal.000 file. These norms start oscillating, until they reach a plateau with a norm = 1/2. Due to the absorption required at the edges of the grids, this norm decreases progressively until zero, giving information on how absorption proceeds and how much remains in the physically relevant region. It should be noted, that only if the propagation is very bad it may present rippling (very bad absorption) or a fast increase (probably because the maximum value energy is not properly set and the scaled Hamiltonian is wrong).

In order to keep the Chebyshev components of the wave packet real, the initial one is built as a linear superposition of incoming and outgoing waves. The outgoing half rapidly evolves towards the edges, resulting in a decrease of the norm from 1/2 to 1/4. The incoming wave packet takes a larger number of iterations to reach the edges, since it has to evolve towards shorter distances and then bounce back.

Outgoing and incoming wave packets may interfere in the initial channel of reactants. To minimize it the parameter **kminelastic** in the elastic probability has to be set to a value where the norm of the component is $\approx 1/4$.

In the typical workflow we create a new folder for each total angular momentum J and copy the **input.dat** file there. We should have the following directory structure:

```
project/
├── input.dat
├── pot/
├── func/
├── J000/
│   └── input.dat
```

Next, we navigate to the **J000** folder and run the MADWAVE3 program as **mpirun -n <number of MPI tasks >/path/to/madwave3/mad3.out**.

The following files are written after execution:

- sal.XYZ: Main output file. Writes the norm of the Chebyshev components at each iteration.
- gaussE: Initial wavepacket in the energy domain. First column is the energy and second the value of the wavefunction.
- gaussR: Initial wavepacket in the position domain. First column is the R coordinate and second the value of the wavefunction.
- distriS2reac.elec{ielec}: Total inelastic probability. Represents energy vs probability.
- distriS2reac.v{v'}.e1: Inelastic probabilities for reactants in v' . The first column is the energy and the subsequent columns are the probabilities for increasing values of $j' = 0, 1, \dots$
- S2prod.v{v_0}.J{j_0}.k{i}: Reaction probabilities in the i th iteration. To see the last results take the largest value of i . First column is the energy, second column the total reaction probability for all the possible product channels. Third is the total probability for reactant and products channel (it should be unity). The fourth is the total reaction probability for the reaction $01 + 2 \rightarrow 02 + 1$ when **iproduct=2**. The subsequent columns present the reaction probability for each of the final vibrational product states for the reaction $01 + 2 \rightarrow 02 + 1$, summed over all the rotational states. Plotting these files provide a good check of the convergence as shown in Fig. 1.
- potr1r2.e{ielec}.j{jelec}: Contains the i elec, j elec matrix element of the PES on the grid. First column is r and the second is R . Subsequent columns are the values of the PES for the various angles in the grid.
- Cvjprod.{i}: Cumulative reaction probability (22).
- prodwv.v{v_0}.Omg{\Omega_0} (if iwrt_pot=1): products rovibrational wavefunction in the vibrational state v_0 represented in a bidimensional grid (r, γ) in reactants Jacobi coordinates.

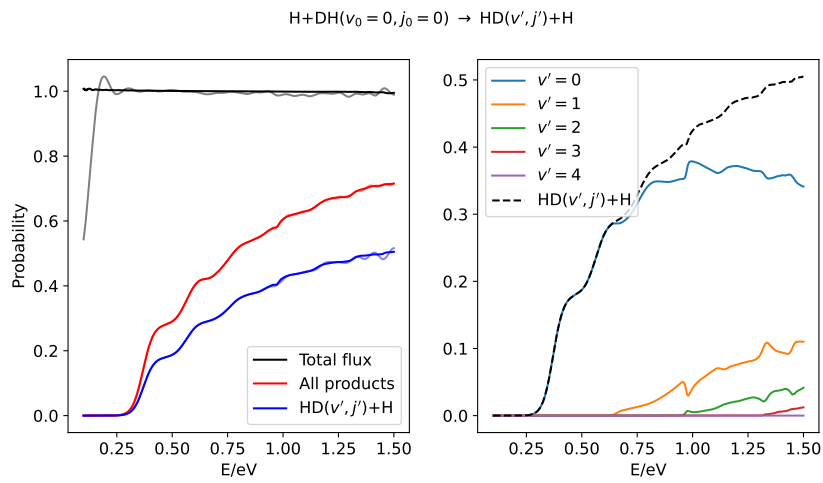


Figure 1: Left panel presents the total flux in black (column 3 of files S2prod.v00.J000.k{i}, total reaction probability (column 2) in red and reaction probability towards the H exchange (column 4) in blue for two different Chebyshev iterations with respect to the energy (column 1). The transparent lines correspond to the second iteration (i=00002) while solid lines correspond to the eight iteration, where convergence has been reached. The right panel breaks down the individual contributions to the total exchange probability in terms of the products vibrational state (columns 5 to 9, for $v' = 0$ to 4).

To resolve the reaction probability for each of the products rotational states the information in the `Cvjprod.{i}` must be reprocessed with the **distri.out** code, producing the **distriS2prod.v{v'}.e1** files with equivalent information to that found in `distriS2reac.v{v'}.e1`.

To further check the convergence of individual state-to-state magnitudes, in Fig. 2 the inelastic (top panel) and reactive (bottom panel) reaction probabilities are compared with hyperspherical time-independent results obtained with the ABC code [3], shown as points. The agreement between the MAD-WAVE3 and ABC results is excellent, what demonstrates the convergence and accuracy achieved with the parameters used (provided in the supplementary information).

6.3. Higher partial wave, $J > 0$, and cross sections

To calculate the other partial waves, J , the number of helicity components has to be determined, $\Omega = \text{IOMMIN}, \dots, \text{IOMMAX}$. In this case, convergence is achieved with $\text{IOMMIN}=0$ and $\text{IOMMAX}=\min(J,7)$. As J increases, the effective rotational barrier increases as well, pushing the reaction probability up towards higher energies as shown in Fig. 3. This shifting is qualitatively well explained by the so called J-shifting approach [39]. However, the shifted results typically overestimate the exact one, producing too large cross sections. An alternative is the so called J-shifting interpolation, in Eq.(23).

The cumulative reaction probabilities, Eq.(22), are calculated with the **crp.out** program, and reads the namelist **sigmaS2prod** in the `input.dat`, in addition to those previously used for the propagations. In this namelist, `Jtotmax` and `nCalc` are the maximum J to be read and the total number of calculated J 's (if all are calculate `nCalc=Jtotmax+1`). An additional file, called **CalculatedJ.dat** is read, with the `nCalc` values of J (first column) and an effective rotational constant B in eV (second column), that optimize the J-shifting interpolation between J_{calc} and $J_{calc} + 1$. These files can be found in the CRP directory in the example.

We need to create a new directory `project/OmgX`, where $X=0, \dots, j_{ref}$, and copy there the reaction probabilities previously calculated into the **JXYZ** files. For $\Omega > 0$, and extra directory p or m have to be added for +1 or -1 parities, respectively. After the execution of the **crp.out** program in the CRP directory, the state-to-state reactive cross sections are written in files **CRP.vfXX.efY**, where XX refers to the final vibrational state of products and Y to the final electronic state. The total cross sections are saved into the **CRPtot.res** files. A similar description for inelastic cross section is valid

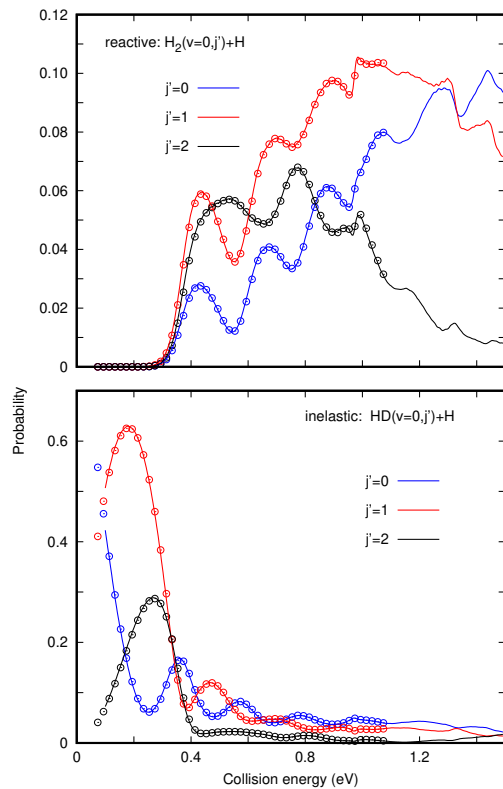


Figure 2: State-to-state probabilities for the $\text{HD}(v = 0, j = 0) + \text{H} \rightarrow \text{HD}(v' = 0, j' = 0, 1, 2) + \text{H}$ inelastic (bottom panel) and $\text{HD}(v = 0, j = 0) + \text{H} \rightarrow \text{H}_2(v' = 0, j' = 0, 1, 2) + \text{D}$ reactive (top panel) collisions for $J=0$. Points are the results obtained with the ABC code, lines are MADWAVE3 results.

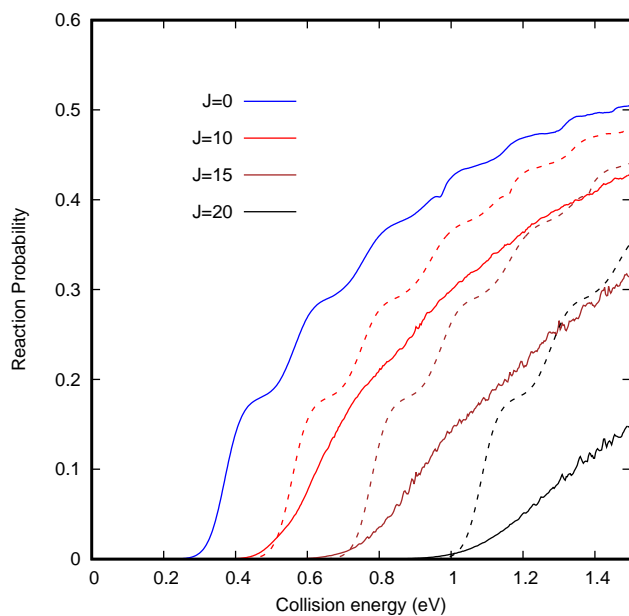


Figure 3: Total H_2 reaction probabilities for several J . Solid lines are MADWAVE3 results, while dashed lines correspond to J-shifting results, *i.e.*, obtained from that of $J = 0$ as $P^J(E) = P^{J=0}(E + J(J + 1))$ [39], where $B = 1.7$ meV is an effective rotational constant.

but in **CIP.vfXX.efY** obtained with the **cip.out** program. In these files, the first column is the collision energy (in eV), the second is $K_0^2(E)$ (in \AA^2), and the remaining are $\mathcal{C}_{v_0 j_0 \Lambda_0, \beta v', j'}(E)$ from $j' = 0, 1, 2, \dots$. Some state-to-state integral cross section are presented in Fig. 4 for reactive and inelastic case.

7. Parallelization efficiency

The most efficient parallelization of this code involves distributing each Ω component of the wave packet across individual processors [1]. Since each Ω is coupled only to adjacent components, $\Omega' = \Omega \pm 1$, this approach limits information transfer to neighboring processors, thereby minimizing communication overhead and maximizing parallelization efficiency.

To accelerate calculations for low to intermediate J values, the grid in the γ angle is also distributed. Due to the L-shape of the grid, not all γ_i values share identical grids in r and R . To balance memory usage and CPU time, the angular grids are distributed non-uniformly.

Defining n_Ω , n_γ and n_{proc} as the number of Ω , the number of angular grid points (nangu in the input) and the number of processors, there are the following restrictions:

$$\begin{cases} \text{if } n_{proc} \leq n_\Omega & \text{mod}(n_\Omega, n_{proc}) = 0 \\ \text{if } n_{proc} > n_\Omega & \begin{cases} n_{proc} = n_\Omega n_{proc}^\gamma \\ \text{mod}(n_{proc}^\gamma, n_\gamma) = 0 \end{cases} \end{cases} \quad (27)$$

meaning that if the number of available processors, n_{proc} , is less than the number of Ω values, then n_{proc} must be a multiple of n_Ω . If the number of processors exceeds the number of Ω values, parallelization will also extend to the γ angles. In this case, the calculation for each γ angle will be distributed across n_{proc}^γ processors, where n_{proc}^γ must be multiple of n_γ .

The use of MPI libraries allows the use of much larger number of processors than OpenMP. Once an optimal value of processor is attributed to MPI, we can proceed to use the shared memory OpenMP parallelization, with a number of threads typically about 2 to 4. For this reason, below we restrict the discussion to parallelization using MPI in different processors (or cores).

The efficiency of the parallelization depends on the size of the packages that need to be transferred among processors. Therefore the efficiency is very dependent on the system, grids and PESs treated. Below we consider the efficiency for the test study presented in section 6. In the output file

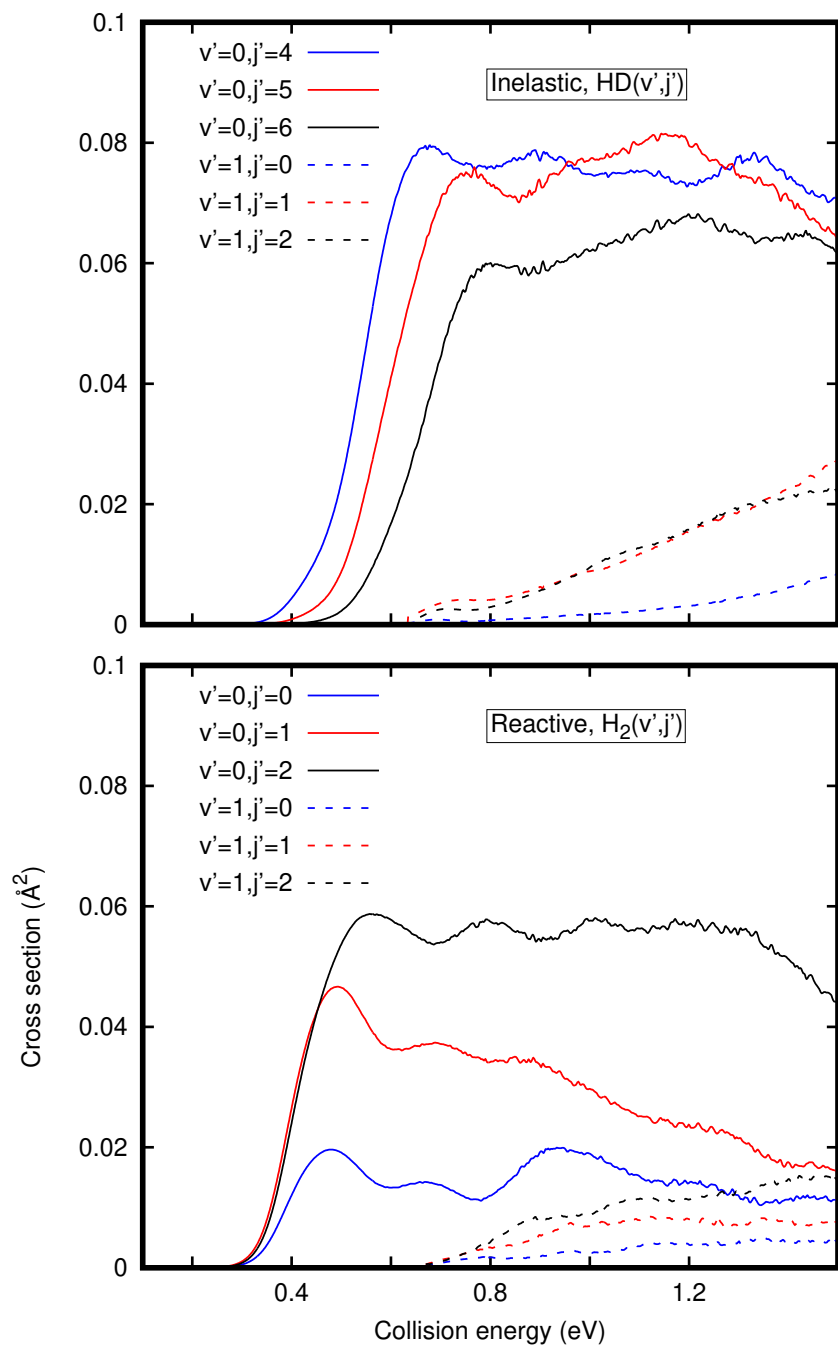


Figure 4: State-to-state cross section for reactive (bottom panel) and inelastic (top panel) for some selected final states of H₂(v', j') and HD(v', j') respectively. Solid lines are for final $v' = 0$, dashed lines for $v' = 1$.

sal.000 the wall time is printed in each loop, consisting on n_{times} Chebyshev iterations.

The parallel speedup is defined as

$$S(n_{\text{proc}}) = \frac{\text{wallclock for serial}}{\text{wallclock for parallel}}, \quad (28)$$

and we consider two cases:

1. $J = 0$ only parallelization over the $n_{\gamma} = n_{\text{angu}} = 140$ angular grid points.
2. $J = 9$, with $\Omega = 0, 1, \dots, 10$, i.e., $n_{\Omega}=10$, where a mixed parallelization over Ω and γ is performed

The parallel speedup is shown in Fig. 5. The calculations were performed in a AMD EPYC GENOA (at 4.05 GHz and 1536 GB of RAM), with 2 nodes of 24 cores each, and the compilation was done with gfortran.

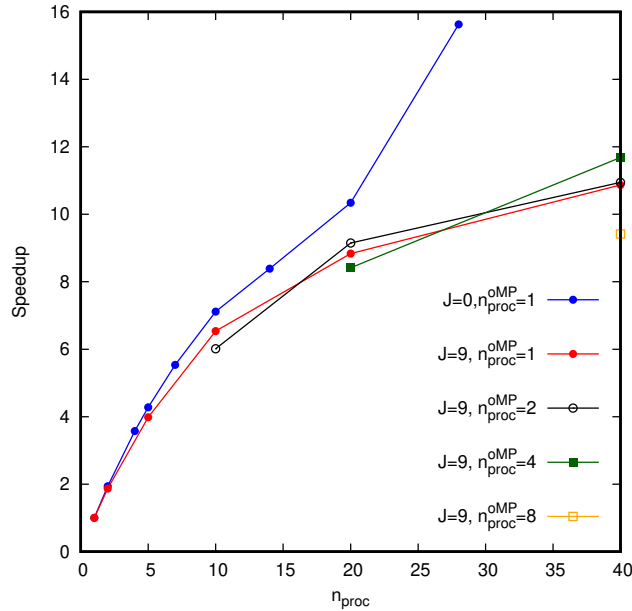


Figure 5: Parallel speedup obtained for $J=0$ ($n_{\Omega} = 1$) and $J=9$ ($n_{\Omega} = 1$), for different number of processors, n_{proc} and $n_{\text{proc}}^{\text{OMP}}$

The speedup for $J = 0$ (blue line) increases continuously up to $n_{\text{proc}} = 20$, presenting an extra-speedup from 20 to 28, just when two nodes are used. In

this case, only MPI parallelization is used. For $J = 10$, the calculations with $n_{\Omega} = 10$ are considerably longer in time, passing from 224 s for $J = 0$ to 3256 s for $J = 10$. Using only MPI, the calculations for $J=10$ presents a lower speedup. This is surprising because the parallelization in Ω is more efficient (the communication is only among sequential cores), and it is probably due to the increase of size of the communication packets.

The efficiency of combining MPI and OpenMP parallelization (keeping constant the total number of cores, n_{proc} , is only shown for $J = 9$, using 1,2 4 and OpenMP threads. For $n_{proc} = 20$ there is a slight increase when using 2 threads, which decreases when using 4. For $n_{proc} = 40$, however, the best speedup is for 4 OpenMP threads, dropping down when using 8 threads.

The overall speedup is dependent on the system and on the computers used, but in general is considered to be satisfactory allowing the use of around 100 cores for large calculations.

8. Conclusions

We have presented the MADWAVE3 program, a FORTRAN90 code devoted to the propagation of quantum wave packets for triatomic systems to compute state-to-state probabilities and cross sections of reactive and inelastic collisional ($A+BC(v,j) \rightarrow AB(v',j')+C$) and photodissociation ($ABC+h\nu \rightarrow A+BC(v,j)$) processes. The program can deal with several coupled electronic states in a diabatic representation. These electronic states are coupled by potential terms, but not by non-adiabatic kinetic terms. The diabatic representation is considered to be diagonal on the reactants' side at long distances while it can be coupled on the products' side.

Several auxiliary codes are distributed within the MADWAVE3 program to analyze and compute different magnitudes such as reactive or inelastic cross sections from the wave packet propagations.

The underlying theoretical background is explained, including the calculation of the reactants' and products' rovibrational states, construction of the initial wave packet, its propagation and analysis of the final wave packet to compute reaction probabilities.

The input structure of the code is presented, as FORTRAN namelists, and an exhaustive description of their variables is indicated in Table 1.

The $D + H_2^+ \rightarrow DH^+ + H$ is presented as an use example of the code and the results compared with those from ABC program.

The code is parallelized using MPI and OpenMP in the helicity Ω and the γ angle between the two Jacobi vectors.

The most updated version of the MADWAVE3 code will always be available at <https://github.com/qmolastro/madwave3>. In its current form it requires the open source libraries for MPI and FFTW3. The source codes, the installation procedure and the example discussed in this work are also provided in the supplementary information as a zip file, in a format close to that found in the github repository.

9. Acknowledgments

We express our gratitude to Carlos Mouriño, from CESGA supercomputer center in Galicia (Spain), for his help in the parallelization of the code, specially in during the implementation the OpenMP when using the non threads-safe library FFTW3. This work has received funding from MICIN (Spain) under Grant Nos. PID2021-122549NB-C21, PID2021-122549NB-C22

References

- [1] O. Roncero, D. Caloto, K. C. Janda, N. Halberstadt, From the sparse to the statistical limit of intramolecular vibrational redistribution in vibrational predissociation: ArCl_2 as an example, *J. Chem. Phys.* 107 (1997) 1406.
- [2] S. Gómez-Carrasco, O. Roncero, Coordinate transformation methods to calculate state-to-state reaction probabilities with wave packet treatments, *J. Chem. Phys.* 125 (2006) 054102.
- [3] D. Skouteris, J. Castillo, D. E. Manolopoulos, Abc: a quantum reactive scattering program, *Comp. Phys. Commun.* 133 (2000) 128.
- [4] H.-D. Meyer, U. Manthe, L. Cederbaum, The multi-configurational time-dependent hartree approach, *Chem. Phys. Lett.* 165 (1990) 73.
- [5] U. Manthe, H.-D. Meyer and L. S. Cederbaum, Wave-packet dynamics within the multiconfiguration Hartree framework: General aspects and application to NOCl , *J. Chem. Phys.* 97 (1992) 3199.
- [6] M. H. Beck, A. Jäckle, G. A. Worth, H.-D. Meyer, The mctdh method: a highly efficient algorithm for propagating wavepackets, *Phys. Rep.* 324 (2000) 1.

- [7] U. Manthe, T. Seideman, W. H. Miller, Full-dimensional quantum mechanical calculation of the rate constant for the $\text{H}_2 + \text{OH} \rightarrow \text{H}_2\text{O} + \text{H}$ reaction, *J. Chem. Phys.* 99 (1993) 10078.
- [8] F. Huarte-Larrañaga, U. Manthe, Full dimensional quantum calculations of the $\text{CH}_4 + \text{H} \rightarrow \text{CH}_3 + \text{H}_2$ reaction rate, *J. Chem. Phys.* 113 (2000) 5115.
- [9] R. Welsch, U. Manthe, Loss of Memory in $\text{H} + \text{CH}_4 \rightarrow \text{H}_2 + \text{CH}_3$ State-to-State Reactive Scattering, *J. Phys. Chem. Lett.* 6 (2015) 338.
- [10] M. Hankel, S. C. Smith, R. J. Allan, S. K. Gray, G. G. Balint-Kurti, State-to-state reactive differential cross sections for the $\text{H} + \text{H}_2 \rightarrow \text{H}_2 + \text{H}$ reaction on five different potential energy surfaces employing a new quantum wavepacket computer code: DIFFREALWAVE, *J. Chem. Phys.* 125 (2006) 164303.
- [11] S. Ghosh, T. Sahoo, S. Adhikari, R. Sharma, A. J. C. Varandas, Coupled 3D Time-Dependent Wave-Packet Approach in Hyperspherical Coordinates: The $\text{D}^+ + \text{H}_2$ Reaction on the Triple-Sheeted DMBE Potential Energy Surface, *J. Phys. Chem. A* 119 (2015) 12392.
- [12] S. Ghosh, R. Sharma, S. Adhikari, A. J. C. Varandas, 3D time-dependent wave-packet approach in hyperspherical coordinates for the $\text{H} + \text{O}_2$ reaction on the CHIPR and DMBE IV potential energy surfaces, *PCCP* 20 (2018) 478.
- [13] S. C. Althorpe, Quantum wavepacket method for state-to-state reactive cross sections, *J. Chem. Phys.* 114 (2001) 1601.
- [14] T. Peng, J. Z. H. Zhang, A reactant-product decoupling method for state to state reactive scattering, *J. Chem. Phys.* 105 (1996) 6072.
- [15] W. Zhu, D. Wang, J. Z. H. Zhang, Quantum dynamics study of $\text{li} + \text{hf}$ reaction, *Theor. Chem. Acc.* 96 (1997) 31.
- [16] J. Dai, J. Z. H. Zhang, Application of reactant-product decoupling method for state to state calculation of $\text{D} + \text{H}_2$ reaction for $J=0$ and 1.

- [17] Y. Shu, H. Zhao, Z. Sun, The Interaction-Asymptotic Region Decomposition Method in Jacobi Coordinates: Triatomic Reactive Scatterings, *J. Phys. Chem. A* 128 (2024) 7982.
- [18] R. Zare, *Angular Momentum*, John Wiley and Sons, Inc., 1988.
- [19] B. Lepetit, D. Lemoine, State-to-state arhbr photodissociation quantum dynamics, *J. Chem. Phys.* 117 (2002) 8676.
- [20] T. González-Lezana, A. Aguado, M. Paniagua, O. Roncero, Quantum approaches for the insertion dynamics of the $H^+ + D_2$ and $D^+ + H_2$ reactive collisions, *J. Chem. Phys.* 123 (2005) 194309.
- [21] R. C. Mowrey, Reactive scattering using efficient time-dependent quantum mechanical wave packet methods on an l-shaped grid, *J. Chem. Phys.* 94 (1991) 7098.
- [22] V. A. Mandelshtam, H. S. Taylor, Spectral projection approach to quantum scattering calculations, *J. Chem. Phys.* 102 (1995) 7390.
- [23] H. Tal-Ezer, R. Kosloff, *J. Chem. Phys.* 81 (1984) 3967.
- [24] Y. Huang, D. J. Kouri, D. K. Hoffman, General, energy-separabl faber polynomial representation of operator functions: theory and application ub quantum scattering, *J. Chem. Phys.* 101 (1994) 10493.
- [25] Y. Huang, S. S. Iyengar, D. J. Kouri, D. K. Hoffman, Further analysis of solutions to the time-independent wave-packet equations of quantum dynamics. ii. scattering as a continuos function of energy using finite, discrete approximate hamiltonians, *J. Chem. Phys.* 105 (1996) 927.
- [26] G. J. Kroes, D. Neuhauser, Performance of a time-independent scattering wave packet technique using real operators and wave functions, *J. Chem. Phys.* 105 (1996) 8690.
- [27] R. Chen, H. Guo, Evolution of quantum system in order domain of chebyshev operator, *J. Chem. Phys.* 105 (1996) 3569.
- [28] S. K. Gray, G. G. Balint-Kurti, Quantum dynamics with real wavepackets, including application to three-dimensional ($J=0$) $D + H_2 \rightarrow HD + H$ reactive scattering, *J. Chem. Phys.* 108 (1998) 950.

- [29] U. V. Riss, H. D. Meyer, Investigation on the reflection and transmission properties of complex absorbing potentials, *J. Chem. Phys.* 105 (1996) 1409.
- [30] M. Paniagua, A. Aguado, M. Lara, O. Roncero, Transition state spectroscopy via infrared excitation of LiHF and LiDF van der waals precursors, *J. Chem. Phys.* 111 (1999) 6712.
- [31] J. Cullum, R. Willoughby, *Lanczos Algorithms for Large Symmetric Eigenvalues Computations*, Birkhäuser, Boston, 1985.
- [32] W. H. Miller, Quantum mechanical transition state theory and a new semiclassical model for reaction rate constants, *J. Chem. Phys.* 61 (1974) 1823.
- [33] D. H. Zhang, J. Z. H. Zhang, Quantum reactive scattering with deep well: time-dependent calculation for $\text{h} + \text{o}_2$ reaction and bound state characterization for ho_2 , *J. Chem. Phys.* 101 (1994) 3672.
- [34] D. Neuhauser, Fully quantal initial-state-selected reaction probabilities ($j=0$) for a four-atom system: $\text{H}_2(v=0, 1, j=0) + \text{oh}(v=0,1, j=0) \rightarrow \text{h} + \text{h}_2\text{o}$, *J. Chem. Phys.* 100 (1994) 9272.
- [35] A. Aguado, M. Paniagua, M. Lara, O. Roncero, Quantum study of the $\text{Li} + \text{HF} \rightarrow \text{LiF} + \text{H}$ reaction, *J. Chem. Phys.* 107 (1997) 10085.
- [36] C. Sanz-Sanz, A. Aguado, O. Roncero, Near-resonant effects in the quantum dynamics of the $\text{H} + \text{H}_2^+$ charge transfer reaction and isotopic variants, *J. Chem. Phys.* 154 (2021) 104104.
- [37] G. G. Balint-Kurti, R. N. Dixon, C. C. Marston, Time-dependent quantum dynamics of molecular photofragmentation processes, *J. Chem. Soc. Faraday Trans.* 86 (1990) 1741.
- [38] S. C. Althorpe, D. J. Kouri, D. K. Hoffman, Further partitioning of the reactant-product decoupling equations of state-to-state reactive scattering and their solution by time-independent wave-packet method, *J. Chem. Phys.* 107 (1997) 7816.
- [39] J. M. Bowman, Reduced dimensionality theories of quantum reactive scattering, *Adv. Chem. Phys.* 61 (1985) 115.

- [40] S. Gómez-Carrasco, O. Roncero, L. González-Sánchez, M. L. Hernández, J. M. Alvariño, M. Paniagua, A. Aguado, Reaction dynamics of $\text{OH}(^2\Pi)+\text{F}(^2P)\rightarrow\text{HF}(^1\Sigma^+)+\text{O}(^3P)$ on the three lower triplet states, *J. Chem. Phys.* 123 (2005) 114310.
- [41] A. Zanchet, T. González-Lezana, A. Aguado, S. Gómez-Carrasco, O. Roncero, Non-adiabatic state-to-state reactive collisions among open shell reactants with conical intersections: the $\text{OH}(^2\Pi)+\text{F}(^2P)$ example, *J. Phys. Chem. A* 114 (2010) 9733.
- [42] E. Aslan, N. Bulut, J. F. Castillo, L. Bañares, F. J. Aoiz, O. Roncero, Accurate time-dependent wave packet study of the $\text{H}++\text{LiH}$ reaction at early universe conditions, *Astrophys. J.* 739 (2012) 31.
- [43] M. B. Krasilnikov, R. S. Popov, O. Roncero, D. D. Fazio, S. Cavalli, V. Aquilanti, O. S. Vasyutinskii, Polarization of molecular angular momentum in the chemical reactions Li plus HF and F plus HD, *J. Chem. Phys.* 138 (2013) 244302.
- [44] A. Zanchet, B. Godard, N. Bulut, O. Roncero, P. Halvick, J. Cernicharo, $\text{H}_2(v=0,1)+\text{C}(^2P)\rightarrow\text{H}+\text{CH}^+$ state-to-state rate constants for chemical pumping models in astrophysical media, *ApJ* 766 (2013) 80.
- [45] A. Zanchet, F. Lique, O. Roncero, J. R. Goicoechea, N. Bulut, Formation of interstellar sh^+ from vibrationally excited H_2 : Quantum study of $\text{S}^+ + \text{H}_2 \rightleftharpoons \text{SH}^+ + \text{H}$ reactions and inelastic collisions, *Astronomy AstroPhys.* 626 (2019) 103.
- [46] A. Zanchet, O. Roncero, E. Karabulut, N. Solem, C. Romanzin, R. Thissen, C. Alcaraz, The role of intersystem crossing in the reactive collision of $\text{S}^+(^4\text{S})$ with H_2 , *J. Chem. Phys.* 161 (2024) 044302.
- [47] C. Sanz, A. van der Avoird, O. Roncero, Collisional and photoinitiated reaction dynamics in the ground electronic state of Ca-HCl, *J. Chem. Phys.* 123 (2005) 64301.
- [48] C. Sanz-Sanz, O. Roncero, R. Hernández-Lamoneda, J. M. Pio, M. A. Taylor, K. C. Janda, Communications: A model study on the electronic predissociation of the NeBr_2 van der waals complex, *J. Chem. Phys.* 132 (2010) 221103.

- [49] N. Bulut, J. Klos, O. Roncero, Quantum mechanical calculations of the state-to-state cross sections and rate constants for the $F+DCl \rightarrow Cl +DF$ reaction, *J. Chem. Phys.* 142 (2015) 214310.
- [50] N. Bulut, O. Roncero, M. Jorfi, P. Honvault, Accurate time dependent wave packet calculations for the $n+ oh$ reaction, *J. Chem. Phys.* 135 (2011) 104307.
- [51] A. Aguado, M. Paniagua, C. Sanz-Sanz, O. Roncero, Transition state spectroscopy of the excited electronic states of Li-HF, *J. Chem. Phys.* 119 (2003) 10088.
- [52] O. Roncero, J. Campos-Martínez, M. I. Hernández, G. Delgado-Barrio, P. Villarreal, J. Rubayo-Soneira, *J. Chem. Phys.* 115 (2001) 2566.
- [53] A. Chenel, O. Roncero, A. Aguado, M. Agúndez, J. Cernicharo, Photodissociation of HCN and HNC isomers in the 7-10 eV energy range, *J. Chem. Phys.* 144 (2016) 144306.
- [54] A. Aguado, O. Roncero, A. Zanchet, M. Agúndez, J. Cernicharo, The photodissociation of HCN and HNC: effects on the HNC/HCN abundance ratio in the interstellar medium, *Astrophys. J.* 838 (2017) 33.
- [55] L. González-Sánchez, S. Gómez-Carrasco, A. Aguado, M. Paniagua, M. L. Hernández, J. M. Alvariño, O. Roncero, Photodetachment spectrum of OHF^- : Three-dimensional study of the heavy-light-heavy resonances, *J. Chem. Phys.* 121 (2004) 309.
- [56] S. Gómez-Carrasco, A. Aguado, M. Paniagua, O. Roncero, Coupled diabatic potential energy surfaces for studying the non-adiabatic dynamics at conical intersections in angular resolved photodetachment simulations of $OHF^- \rightarrow OHF + e^-$, *J. Chem. Phys.* 125 (2006) 164321.
- [57] F. T. Smith, Diabatic and adiabatic representations for atomic collision problems, *Phys. Rev.* 179 (1969) 111.
- [58] M. Baer, Electronic non-adiabatic transitions. derivation of the general adiabatic-diabatic transformation matrix, *Mol. Phys.* 40 (1980) 1011.
- [59] C. A. Mead, D. G. Truhlar, Conditions for the definition of a strictly diabatic electronic basis for molecular systems, *J. Chem. Phys.* 77 (1982) 6090.

- [60] H. Köppel, W. Domcke, L. Cederbaum, Multimode molecular dynamics beyond the born-oppenheimer approximation, *Adv. Chem. Phys.* 57 (1984) 59.
- [61] A. Thiel, H. Köppel, Proposal and numerical test of a simple diabaticization scheme, *J. Chem. Phys.* 110 (1999) 9371.
- [62] H. Köppel, Diabatic representation: methods for the construction of diabatic electronic states, in: D. Y. W. Domcke, H. Köppel (Eds.), *Conical Intersections: electronic structure, dynamics and spectroscopy*, Advanced series in Physical Chemistry, World Scientific Publishing Co., 2004, p. 175.
- [63] H. G. abd D. R. Yarkony, Accurate non-adiabatic dynamics, *PCCP* 18 (2016) 26335.
- [64] K. Naskar, S. Mukherjee, B. Mukherjee, S. Ravi, S. Mukherjee, S. Sardar, S. Adhikari, ADT: A Generalized Algorithm and Program for Beyond Born-Oppenheimer Equations of N Dimensional Sub-Hilbert Space, *J. Chem. Theo. Comput.* 16 (2020) 1666.
- [65] A. Aguado, O. Roncero, C. Sanz-Sanz, Three states global fittings with improved long range: singlet and triplet states of H_3^+ , *PCCP* 23 (2021) 7735.